

## Resistivity dominated by surface scattering in sub-50 nm Cu wires

R. L. Graham,<sup>1</sup> G. B. Alers,<sup>1,a)</sup> T. Mountsier,<sup>2</sup> N. Shamma,<sup>2</sup> S. Dhuey,<sup>3</sup> S. Cabrini,<sup>3</sup>  
R. H. Geiss,<sup>4</sup> D. T. Read,<sup>4</sup> and S. Peddetti<sup>5</sup>

<sup>1</sup>Department of Physics, University of California, Santa Cruz, California 95064, USA

<sup>2</sup>Novellus Systems, San Jose, California 95134, USA

<sup>3</sup>Molecular Foundry, Lawrence Berkeley National Laboratory, University of California, Berkeley, California 94710, USA

<sup>4</sup>National Institute of Standards and Technology, Boulder, Colorado 80305, USA

<sup>5</sup>Department of Chemical and Biomolecular Engineering, Clarkson University, Potsdam, New York 13676, USA

(Received 10 September 2009; accepted 21 December 2009; published online 29 January 2010)

Electron scattering mechanisms in copper lines were investigated to understand the extendibility of copper interconnects when linewidth or thickness is less than the mean free path. Electron-beam lithography and a dual hard mask were used to produce interconnects with linewidths between 25 and 45 nm. Electron backscatter diffraction characterized grain structure. Temperature dependence of the line resistance determined resistivity, which was consistent with existing models for completely diffused surface scattering and line-edge roughness, with little contribution from grain boundary scattering. A simple analytical model was developed that describes resistivity from diffuse surface scattering and line-edge roughness. © 2010 American Institute of Physics.

[doi:10.1063/1.3292022]

Extending copper interconnect technology will be of critical importance for achieving continued increases in density for both memory and logic circuits. As feature size shrinks, surface scattering and smaller grain size can lead to increased resistivity.<sup>1,2</sup> The mean free path  $\lambda$  (MFP) of electrons in copper<sup>3</sup> is 39 nm; this letter reports on copper lines of approximately this size.

Resistivity in metal is due to electron scattering, where the total scattering rate is a sum of the rates due to different scattering sources. Electrons scatter when they absorb or emit phonons,<sup>4</sup> reach the line surface,<sup>5</sup> reflect at the boundary of a grain,<sup>6</sup> or encounter impurities in metal and metal alloys.<sup>7</sup> Copper resistivity due to electron-phonon interaction depends linearly on temperature between 100 and 400 K, while the resistivities due to other mechanisms (scattering at line surfaces, grain boundaries, and impurities) do not vary with temperature,<sup>2</sup> have similar geometry-dependence,<sup>5,6</sup> and can be difficult to separate from each other.

The Fuchs model<sup>5</sup> for surface scattering relates the conductivity  $\sigma$  of a narrow line to the bulk conductivity  $\sigma_0$  for the cases of completely inelastic and partially elastic scattering at the surfaces. Chambers<sup>8</sup> found the conductivity of thin metal films and wires to differ only by the effective cross-section, which simplifies to the result that Fuchs found for a thin film.

Copper interconnects can be considered to have a rectangular cross-section and an essentially infinite length. Using the angles defined by Josell *et al.*,<sup>9</sup> Zhang *et al.*,<sup>3</sup> applied conductivity relationships derived by Fuchs and Chambers to rectangular geometry. By following the same procedure as Zhang *et al.*, the diffuse surface scattering contribution to conductivity  $\sigma/\sigma_0$  for a rectangular wire of width  $w$  and height  $h$  can be written as

$$\begin{aligned} \frac{\sigma}{\sigma_0} = & 1 - \frac{6}{4\pi wh} \int_0^w dx \int_0^h dy \int_{-\tan^{-1}\left(\frac{y}{x}\right)}^{\tan^{-1}\left(\frac{h-y}{x}\right)} d\phi \\ & \times \int_0^\pi d\theta \sin\theta \cos^2\theta e^{\left(\frac{-x}{\lambda \sin\theta \cos\phi}\right)} \\ & - \frac{6}{4\pi wh} \int_0^w dx \int_0^h dy \int_{-\tan^{-1}\left(\frac{x}{h-y}\right)}^{\tan^{-1}\left(\frac{w-x}{h-y}\right)} d\phi \\ & \times \int_0^\pi d\theta \sin\theta \cos^2\theta e^{\left(\frac{-(h-y)}{\lambda \sin\theta \cos\phi}\right)}. \end{aligned} \quad (1)$$

The conductivity in this form can be integrated numerically for particular values of height and width.

A simple model is proposed that supposes that the inverse-height dependence of thin-film resistivity<sup>10</sup> can be modified for narrow lines by including an inverse-width dependence. The ratio of resistivity  $\rho$  to bulk resistivity  $\rho_0$  can be approximated as

$$\left(\frac{\rho}{\rho_0}\right) = 1 + K\left(\frac{\lambda}{w} + \frac{\lambda}{h}\right), \quad (2)$$

where  $K$  is a fitting constant. The unity term corresponds to the bulk resistivity dominated by phonon scattering. We find that Eq. (2) can be fit within 5% to the numerical solution of Eq. (1) for  $K=0.46$ . Figure 1 shows this fit for heights ranging from 10 to 100 nm and aspect ratio (defined as height divided by width) between 0.25 and 4 (appropriate for standard semiconductor fabrication). The simple model calculates resistivity due to surface scattering and bulk metal quickly and without the need for numerical integration.

The Mayadas and Shatzkes (MSJ) model<sup>5</sup> estimates the effects of grain surfaces on electron scattering and the resulting change in metallic conductivity. By equating the average grain diameter  $D$  with the distance  $d$  between grain boundaries, MSJ derive a simple expression for the ratio of con-

<sup>a)</sup>Electronic mail: galers@ucsc.edu.

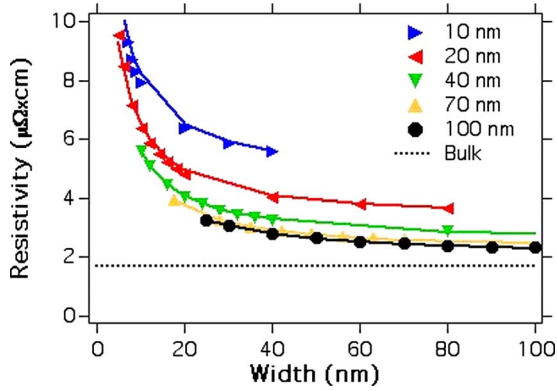


FIG. 1. (Color online) Comparison of resistivity in narrow lines, as calculated from both the surface scattering model [lines, Eq. (1)] and the simple model [points, Eq. (2)] for line thicknesses between 10 and 100 nm and aspect ratios between 0.25 and 4.

ductivity due to grain surfaces  $\sigma_g$  to bulk conductivity  $\sigma_0$ . Studies of thin metal films show that grain boundary scattering dominates the increase in resistivity in two-dimensional systems.<sup>11,12</sup>

An additional source of geometry-dependent resistance is cross-sectional area fluctuations due partially to line edge roughness (LER) as discussed by Ercius *et al.*<sup>13</sup> The simplest model for resistance increase from LER is a purely geometrical reduction in cross-sectional area by narrow portions of the line. This does not impact the intrinsic resistivity, but narrow portions of the line will preferentially increase resistance when summed together. Area variations from LER have a Gaussian distribution,<sup>14</sup> and this can be accounted for with a multiplicative factor in Eq. (2) that averages over all width variations along the line, such that

$$\left(\frac{\rho}{\rho_0}\right) = \left[1 + K\left(\frac{\lambda}{w} + \frac{\lambda}{h}\right)\right] \frac{\langle A \rangle}{s\sqrt{2\pi}} \int_{\varepsilon}^{\infty} \left(\frac{1}{A}\right) \times \exp\left[-\frac{(A - \langle A \rangle)^2}{2s^2}\right] dA, \quad (3)$$

where  $A = hw$  is the cross-sectional area,  $\langle A \rangle$  is the mean area,  $s$  is the standard deviation in area, and  $0 < \varepsilon \ll 1$ . This model assumes that scattering is completely diffused and that the electron scatters with a random angle relative to the sidewalls.<sup>15</sup>

Conventional 300 mm fabrication and metallization tools were used to form single-damascene copper lines and vias. A dielectric stack of 100 nm tetraethyl orthosilicate (TEOS-SiO<sub>2</sub>), 100 nm ashable hard mask (AHM), 35 nm SiN hard mask, and 100 nm poly-methyl methacrylate (PMMA) resist was deposited on a silicon wafer with plasma-enhanced chemical vapor deposition. Electron-beam lithography was used to pattern the PMMA with 20 to 60 nm features. Reactive ion etching was used to transfer this pattern to the SiN hard mask, remove the resist, and then transfer the SiN pattern into the AHM. The use of a dual hard mask reduced LER after the final etching into TEOS-SiO<sub>2</sub>. The Ta barrier and Cu seed layers were deposited by physical vapor deposition, and Cu plating was done by electrochemical deposition (ECD) followed by an anneal at 150 °C for 60 min. Chemical-mechanical polishing was performed to remove the Cu overburden, and some final manual polishing produced electrically testable lines less than 50 nm wide.

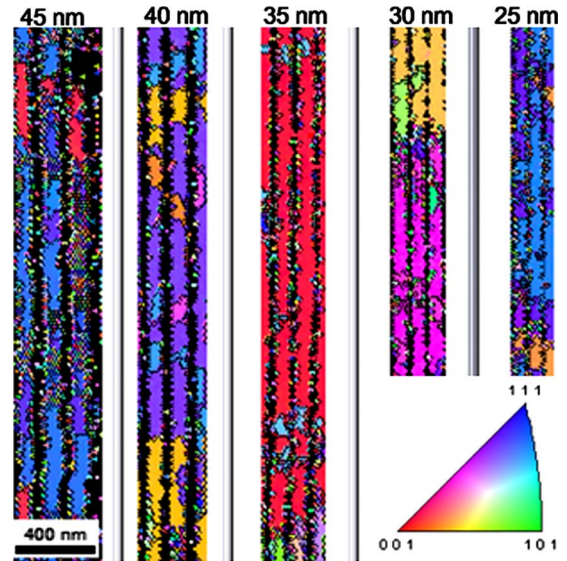


FIG. 2. (Color online) EBSD data of large grains and correlated grain orientation in three adjacent Cu lines with widths (from left) 45, 40, 35, 30, and 25 nm and with a Ta barrier. Line colors correspond to the orientation normal to the sample surface, according to the triangle.

Grain structure depends largely on preparation conditions, especially during the metallization steps of barrier and Cu deposition.<sup>7,10</sup> The resistivity due to Cu grain surfaces, according to the MSJ model, depends on the ratio of the MFP to the average grain size. The grain size  $d$  and wire diameter  $D$  are regularly equated when data are fitted to existing resistivity models,<sup>6,16</sup> which is not always a valid assumption. Grain size and crystal orientation were characterized by electron backscatter diffraction (EBSD). By use of a 20 kV incident electron beam with penetration depth of 20 to 30 nm, EBSD was used to map the orientations of the grains in the individual lines. Each EBSD scan mapped  $0.026 \times 1.0 \mu\text{m}^2$  in 10 nm steps. Grains with dimensions ranging from 30 to 800 nm along the lines were observed for line-widths between 25 and 45 nm.

The lines predominantly had a bamboo structure, with observed copper grains filling the width and height of the lines and with grain boundaries perpendicular to the line axis. The EBSD data in Fig. 2 show areas of well-defined crystal structure (areas with only one color) spanning the entire width of the line. The EBSD results also show that grains in adjacent lines often have the same orientation, which suggests that grain structures in the lines are remnants of larger grain structure in the overplating after ECD and annealing<sup>10</sup> and contradicts the theory that grain growth is limited by the geometry of the wire.<sup>17</sup> According to the MSJ model, if grain size is much larger than the MFP, then grain size is not important for scattering. For 35 nm width lines, the average grain size was 100 nm, with a standard deviation of 120 nm.<sup>18</sup> All of the line images in Fig. 2 show very large grains that are much larger than either the width or the height of the Cu wires and that suggest that the assumption  $d = D$  is not valid for these wires.

The total resistivity  $\rho$  can be written as a sum of the resistivities due to the temperature-dependent scattering mechanism (phonon scattering  $\rho_p$ ) and the residual, nontemperature-dependent mechanisms.<sup>1,3</sup> In that case, the partial derivative of resistance with respect to temperature can be used to separate the resistivity and cross-sectional

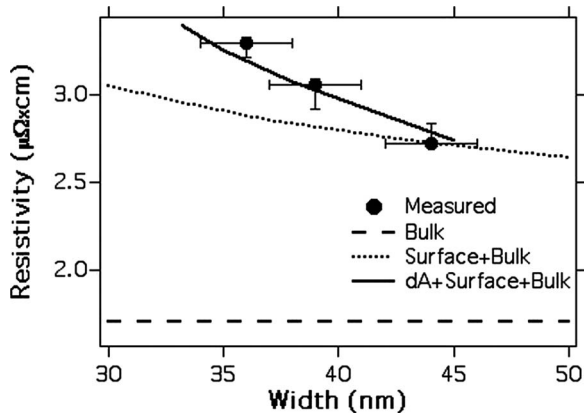


FIG. 3. Resistivities of 100 nm thick Cu lines determined by resistance measurements (points) at 30 °C compared with the resistivity models for phonon and surface scattering [dotted, Eq. (2)], the added impact of area variations [solid, Eq. (3)], and the resistivity of bulk Cu (dashed).

area from resistance versus temperature measurements. The results for resistivity are plotted in Fig. 3 along with the values calculated with Eq. (2), assuming contributions from only phonons and surface scattering for  $T=30$  °C and  $\rho_0 = 1.7 \mu\Omega \text{ cm}$ .

For widths above 40 nm, the magnitude of the measured resistivities is consistent with completely diffused surface scattering. Diffused scattering has been reported for Cu/Ta interfaces because of the mismatch of the Fermi surfaces at the surface of the wire<sup>19</sup> and for Cu films that were annealed as thick films and subsequently thinned by CMP.<sup>10,20</sup> The resistivity at the smallest dimension, and the increase in resistivity for decreasing width, is inconsistent with phonon and surface scattering alone, given by Eq. (2).

Area fluctuations in a fully processed damascene line come from many sources including lithography, etch, Ta barrier roughness, and surface roughness. Scanning electron microscopy and atomic force microscopy analysis on these 35 nm lines yielded an estimated variation of 6 nm in width (600 nm<sup>2</sup> in area), primarily from PMMA erosion during etch, and 3 nm of surface roughness (105 nm<sup>2</sup> in area). The amount of area variation  $dA$  required to account for the measured excess effective resistivity in equation Eq. (3) is 900 nm<sup>2</sup> and is shown in Fig. 3. Ercius *et al.*<sup>13</sup> measured 500 nm<sup>2</sup> area fluctuations in 80 nm wide copper damascene lines, due in part to fluctuations in the two-dimensional profile of the trench and the Cu/Ta interface, not just the LER. LER and profile variations are expected to be larger with PMMA than with deep ultraviolet resists, due to greater erosion, making 900 nm<sup>2</sup> plausible. The horizontal error bars in Fig. 3 represent uncertainties in measuring the *mean* line width of  $\pm 2$  nm. The vertical error bars in Fig. 3 represent an average of resistance measurements over several days. Due to the test structure layout, four-point resistance measurements were not available for the 25 and 50 nm wires.

Resistivity in small metal wires is due primarily to electron scattering within the metal and at its surfaces. In the experiment, wires with widths from 35 to 45 nm were fabricated, their crystal structures were analyzed, and their resis-

tances were measured at different temperatures. The grain size along the length of the Cu line was generally much larger than the dimension of the line cross-section, suggesting that grain boundary scattering did not contribute significantly to increased resistivity in these wires. Measurements of line resistance at different temperatures were used to calculate resistivities, which were compared to the existing model for surface scattering. For line widths above 40 nm, the magnitude of measured resistivities is consistent with completely diffuse surface scattering and phonon scattering. Below 40 nm, the impact of LER was included assuming a Gaussian variation in area along the length of the line. This experimental work has extended the understanding of copper damascene grain growth to sub-50 nm lines. Conventional 300 mm metallization methods were shown to be extendible to sub-30 nm feature sizes.

Portions of this work were performed at the Molecular Foundry, Lawrence Berkeley National Laboratory, which is supported by the Office of Science, Office of Basic Energy Sciences, of the U.S. Department of Energy under Contract No. DE-AC02-05CH11231. Portions of this work were supported by the NIST Office of Microelectronics Programs under Project No. 2004-012.

- <sup>1</sup>D. Josell, S. H. Brongersma, and Z. Tokei, *Annu. Rev. Mater. Res.* **39**, 231 (2009).
- <sup>2</sup>G. Steinlesberger, M. Engelhardt, G. Schindler, W. Steinhögl, A. von Glasow, K. Mosis, and E. Bertagnolli, *Microelectron. Eng.* **64**, 409 (2002).
- <sup>3</sup>W. Zhang, S. H. Brongersma, Z. Li, D. Li, O. Richard, and K. Maex, *J. Appl. Phys.* **101**, 063703 (2007).
- <sup>4</sup>J. J. Plombon, E. Andideh, V. M. Dubin, and J. Maiz, *Appl. Phys. Lett.* **89**, 113124 (2006).
- <sup>5</sup>K. Fuchs, *Math. Proc. Cambridge Philos. Soc.* **34**, 100 (1938).
- <sup>6</sup>A. F. Mayadas, M. Shatzkes, and J. F. Janak, *Appl. Phys. Lett.* **14**, 345 (1969).
- <sup>7</sup>W. Zhang, S. H. Brongersma, N. Heylen, G. Beyer, W. Vandervorst, and K. Maex, *J. Electrochem. Soc.* **152**, C832 (2005).
- <sup>8</sup>R. G. Chambers, *Proc. R. Soc. London, Ser. A* **202**, 378 (1950).
- <sup>9</sup>D. Josell, C. Burkhard, Y. Li, Y.-W. Cheng, R. R. Keller, C. A. Witt, D. R. Kelley, J. E. Bonevich, B. C. Baker, and T. P. Moffat, *J. Appl. Phys.* **96**, 759 (2004).
- <sup>10</sup>G. B. Alers, J. Sukamto, S. Park, G. Harm, and J. Reid, *Semicond. Int.* **29**, 38 (2006).
- <sup>11</sup>J. Homoth, M. Wenderoth, T. Druga, L. Winking, R. G. Ulbrich, C. A. Bobisch, B. Weyers, A. Bannani, A. M. Bernhart, M. R. Kaspers, and R. Moller, *Nano Lett.* **9**, 1588 (2009).
- <sup>12</sup>M. A. Schneider, M. Wenderoth, A. J. Heinrich, M. A. Rosentreter, and R. G. Ulbrich, *Appl. Phys. Lett.* **69**, 1327 (1996).
- <sup>13</sup>P. Ercius, L. M. Gignac, C.-K. Hu, and D. A. Muller, *Microscopy and Analysis* **15**, 244 (2009).
- <sup>14</sup>D. Drygiannakis, G. P. Patsis, I. Raptis, D. Niakoula, V. Vidali, E. Coula-douros, P. Argitis, and E. Gogolides, *Microelectron. Eng.* **84**, 1062 (2007).
- <sup>15</sup>D. Josell, *J. Appl. Phys.* **100**, 123705 (2006).
- <sup>16</sup>W. Steinhögl, G. Schindler, G. Steinlesberger, and M. Engelhardt, *Phys. Rev. B* **66**, 075414 (2002).
- <sup>17</sup>W. Zhang, S. H. Brongersma, T. Conard, W. Wu, M. Van Hove, W. Vandervorst, and K. Maex, *Electrochem. Solid-State Lett.* **8**, C95 (2005).
- <sup>18</sup>R. H. Geiss, D. T. Read, G. B. Alers, and R. L. Graham, *AIP Conf. Proc.* **1173**, 154 (2009).
- <sup>19</sup>S. M. Rossnagel and T. S. Kuan, *J. Vac. Sci. Technol. B* **22**, 240 (2004).
- <sup>20</sup>W. Zhang, S. H. Brongersma, T. Clarysse, V. Terzieva, E. Rosseel, W. Vandervorst, and K. Maex, *J. Vac. Sci. Technol. B* **22**, 1830 (2004).